Exposure to Titanium Dioxide Nanomaterials Provokes Inflammation of an *in Vitro* Human Immune Construct

Brian C. Schanen,[†,§] Ajay S. Karakoti,[‡] Sudipta Seal,[‡] Donald R. Drake III,[†] William L. Warren,[†] and William T. Self[§,*]

[†]VaxDesign Corporation, 12612 Challenger Parkway, Suite 365, Orlando, Florida 32826, [‡]Advanced Materials Processing and Analysis Centre (AMPAC), Department of Mechanical, Materials and Aerospace Engineering (MMAE), Nanoscience and Technology Center (NSTC), and [§]Department of Molecular Biology and Microbiology, Burnett School of Biomedical Science, UCF College of Medicine

ABSTRACT Nanoparticle technology is undergoing significant expansion largely because of the potential of nanoparticles as biomaterials, drug delivery vehicles, cancer therapeutics, and immunopotentiators. Incorporation of nanoparticle technologies for *in vivo* applications increases the urgency to characterize nanomaterial immunogenicity. This study explores titanium dioxide, one of the most widely manufactured nanomaterials, synthesized into its three most common nanoarchitectures: anatase (7—10 nm), rutile (15—20 nm), and nanotube (10—15 nm diameters, 70—150 nm length). The fully human autologous MIMIC immunological construct has been utilized as a predictive, nonanimal alternative to diagnose nanoparticle immunogenicity. Cumulatively, treatment with titanium dioxide nanoparticles in the MIMIC system led to elevated levels of proinflammatory cytokines and increased maturation and expression of costimulatory molecules on dendritic cells. Additionally, these treatments effectively primed activation and proliferation of naïve $CD4^+$ T cells in comparison to dendritic cells treated with micrometer-sized (>1 μm) titanium dioxide, characteristic of an *in vivo* inflammatory response.

KEYWORDS: nanoparticles · titanium dioxide · toxicology · human · inflammation

Nanomaterials, particles with diameters of less than 100 nm, have been rapidly assimilated into the consumer market because of their unique physiochemical properties and tunable characteristics. Nanoscale titanium dioxide (TiO_2), one of the most widely manufactured nanoparticles, has been incorporated into pigments, cosmetics, sunscreens, and is at the frontier of nanotechnology with its application as a biomaterial. For instance, nanostructured TiO_2 has been utilized in dental implant technology and is being widely studied for various biomedical applications including scaffolds, coatings, and implants.[1,2] Nanoscale TiO_2 has also gained significant interest in the field of tissue engineering, providing researchers with the ability to repair, replace, or even enhance normal tissue function.

While these results show significant promise, there are conflicting reports on the exposure risk of nanoparticles and their degradation products to humans. For example, nanostructured TiO_2, a biocompatible coating for grafts and a potential suitable bone substitute,[3,4] has been implicated in cell culture, animal, and epidemiological studies to promote pulmonary disease and the development of cancer.[5−10] A catalog of similar hazardous findings has led to the classification of nanoscale TiO_2 as a potential carcinogen by the International Agency for Research on Cancer (IARC).[11−13] Nanoscale TiO_2 might elicit inflammation *via* the release of innate immune triggers, such as reactive oxygen species, or otherwise being recognized as a foreign entity by the host.[14,15] However, a scarcity of information on the interaction of these agents with cells of the human immune system exists, likely a result of the current deficit of appropriate assays to evaluate human immunity in the laboratory. This underlines the need for novel approaches using predictive assay models focused on the human inflammatory response to determine the impact on biological systems and human health.

We undertook an extensive set of studies to develop a sensitive and reliable model to evaluate human immunity in the laboratory. This system, termed modular immune *in vitro* construct (MIMIC), comprises several components that permit the interrogation of innate (short-term inflammatory) and adaptive (long-term memory) immune responses in separate or longitudinal studies. The peripheral tissue equivalent (PTE) component of the MIMIC system is principally composed of blood vein endothelial cells, which participate in inflammatory reactions by secreting soluble factors and regulating the flow of immune cells from the vasculature into tissues, and monocyte-derived

*Address correspondence to wself@mail.ucf.edu.

Received for review April 23, 2009 and accepted August 11, 2009.

Published online August 19, 2009.
10.1021/nn900403h CCC: $40.75

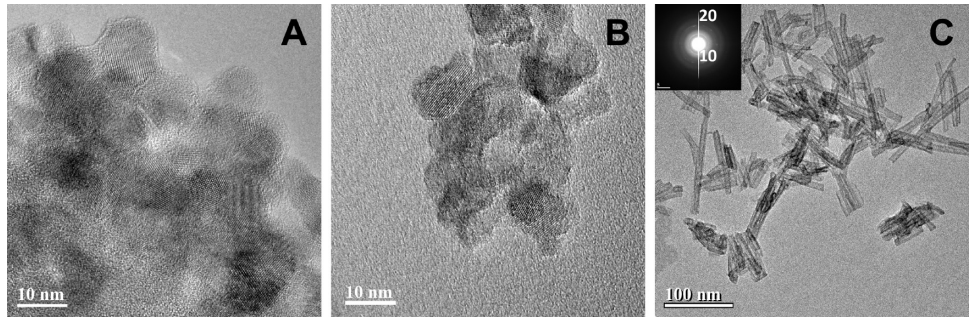

Figure 1. HRTEM image of titania nanoparticles (A) anatase, (B) rutile, and (C) nanotubes. Partially amorphous character of particles is observed in case of anatase nanoparticles, while the aspect ratio of nanotubes was around 1:10 to 1:15.

dendritic cells (DCs), a critical antigen presenting cell population that bridges innate and adaptive responses and stimulates naïve T-cell responses. The synergistic effect of the cell types comprising the PTE permits evaluation of early immune responses associated with foreign body encounter and acquisition and has been shown to support the induction of inflammatory responses against a variety of immunostimulators and immunosuppressants.[16−19]

Here, we employed the PTE construct of the MIMIC system to enumerate and characterize the capacity of TiO_2 formulations (anatase, rutile, and nanotubes) to induce inflammation. We have chosen to study multiple crystal phases of nanoscale TiO_2 because of conflicting biocompatibility reports despite widespread incorporation into the consumer market.[1,3,4,20−26] These assays revealed that treatment with these TiO_2 formulations generate ROS production, increase proinflammatory cytokine expression from the endothelium and DC population, increase DC maturation, and have the capacity to trigger activation and proliferation of $CD4^+$ T cells. This study has emphasized the utility of MIMIC for testing the efficacy and immunotoxicity of nanomaterials and determined that these TiO_2 nanoparticle formulations induce inflammation.

RESULTS AND DISCUSSION

Particle Characteristics. TiO_2 for commercial or tissue engineering applications is commonly prepared as either nanotubes or one of two crystal phases (rutile and anatase). Therefore, these three types of nanostructures were prepared for use in this study. Consistent and optimal material architecture began with the controlled synthesis of TiO_2 nanotubes and nanoparticles using simple wet chemical and hydrothermal synthesis. The structure and diameter of each material was verified using high resolution transmission electron microscopy (HRTEM) (Figure 1). Anatase nanoparticles were between 7−10 nm wide, while the rutile nanoparticles were 15−20 nm in diameter. The hydrothermally synthesized titania nanotubes shown in Figure 1C were approximately 10−15 nm in diameter and 70−150 nm in length. All nanomaterials were prepared in a single batch to ensure confidence in material consistency throughout the experiments shown here. Since these preparations were being used in immunoassays (see below), great effort was taken to ensure they were free of contaminating lipopolysaccharide (LPS); all samples were confirmed negative for endotoxin (EU $<$ 0.6) using the quantitative kinetic chromogenin Limulus Amoebocyte Lysate method (data not shown).

Particle Dosing. Because many TiO_2 nanomaterial applications require direct (*in vivo*) or indirect (environmental) human exposure, it is important to understand the impact of these materials on human health. As a first gauge of the impact of TiO_2 nanoparticles on human physiology, we evaluated the toxicity of these products on the two cell types (HUVECs and PBMCs) comprising the PTE construct using a 3-(4,5-dimethylthiazol-2-yl)-2,5-diphenyltetrazolium bromide (MTT) reduction assay in which viable cells form a colorimetric signal *via* enzymatic modification of the MTT substrate. The cells were treated with 2-fold dilutions of nanoparticles between 0.05 and 100 μM, and viability was normalized by setting the average recovery of cells in an untreated control to 100%. At the highest concentration (100 μM), nanoparticles were toxic to HUVEC, resulting in an average viability of 44% for all three formulations after a 48-h treatment (Figure 2A). This data was consistent with our preliminary studies using the human adenocarcinoma line, A549, and a keratinocyte line, HaCaT (data not shown). PBMCs, on the other hand, were routinely more resistant to TiO_2 nanoparticles, as treatment with equivalent concentrations of nanoparticles resulted in an average cell viability of 83% for all three formulations (Figure 2B). In both cell types, the toxicity of nanoparticles was reasonably consistent over a broad dose range (25−100 μM), while cell recovery was markedly improved at nanoparticle concentrations equal to or less than 1.56 μM. In an effort to confirm these observations, we evaluated the same particle-dosing panel with an assay that relies on a colorimetric readout of the release of lactate dehydrogenase (LDH) from the cell cytosol into the culture supernatant following disruption of the plasma membrane. Using this approach, we were surprised to find that the loss of cell viability remained below 18% for both HUVEC and PBMCs in all dosing regimens (Figure 2C,D), which

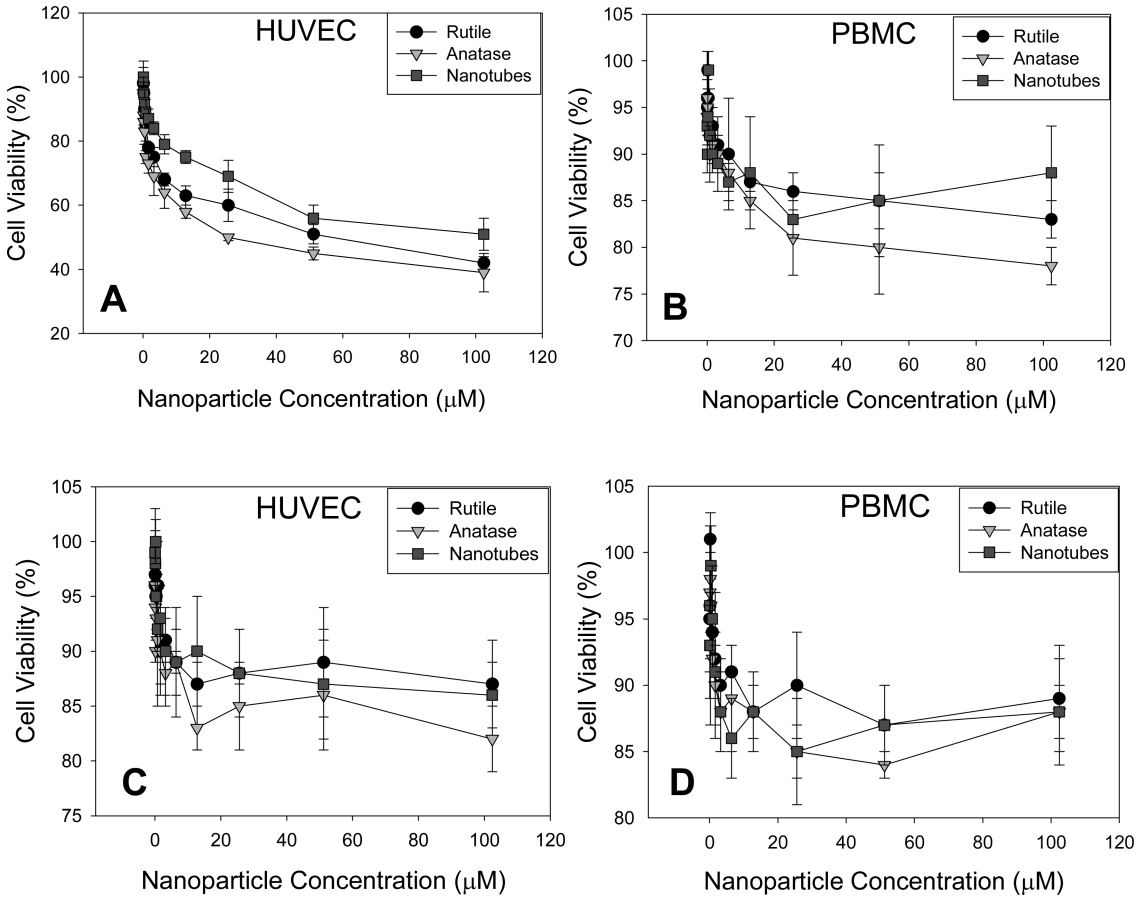

Figure 2. Toxicity of TiO_2 nanomaterials in HUVEC and PBMC primary culture models. (A) HUVEC cells cultured in medium 199 containing 20% serum and (B) PBMCs cultured in X-VIVO-15 were exposed to TiO_2 nanoparticles at concentrations indicated in the plot. MTT dye reduction was assessed after incubating the cells with the nanomaterials for 24 h, and the absorbance collected was compared to untreated cells to determine the relative percent cell viability. The cells were prepared in the same manner as described above and measured for LDH release by loss of cell membrane integrity after 24 h nanoparticle treatment. Both the (C) HUVEC cells and (D) PBMC coculture did not have a sharp reduction in viability as measured by absorbance from the LDH reaction. Error bars represent mean ± SD for at least three independent experiments.

suggests that titanium nanoparticles reduce cellular metabolic activity (Figure 2A,B) but do not trigger overt cell destruction/necrosis (Figure 2C,D). The release of LDH represents death of the cell and release of cytosolic contents into the extracellular environment, whereas MTT reduction is more a sign of metabolic activity and reductive capacity. The differences in measured endothelial cell viability between the MTT assay (44%) and the LDH assay (82%) suggests that chronic exposure to TiO_2 nanomaterials may affect metabolism at doses that do not cause cell death. Although these results may have implications in terms of nanoparticle exposure, our goal was to determine a dosing regimen that would not result in overt toxicity to the relevant cell models, and thus we chose doses at levels that were not significantly affecting viability by either end point.

Innate Response Induced by Nanoparticle Treatment. The innate immune system comprises a number of cell types that respond by recognition of nonself antigens *via* pattern recognition receptors and pathogen-associated molecular patterns resulting in the rapid release of a variety of pro-inflammatory factors.[27,28] For example, IL-1α, IL-1β, IL-6, and TNFα direct the innate response by recruiting and activating neighboring immune cells. Here, we sought to evaluate inflammatory responses induced by TiO_2 nanomaterials. We employed the PTE construct, because, as highlighted above, it was designed to replicate DC differentiation/recruitment and inflammatory responses in human skin. Since this analysis requires functioning, metabolically active cells, we chose to work with nanoparticles at a dose of 1.56 μM, which triggered no more than 17% cell death in studies outlined above (Figure 2A−D).

For this analysis, the PTE construct was treated with nanoparticles for 48 h before supernatants were collected and analyzed by a multiplex cytokine array for the expression of inflammatory cytokines. When treated with nanoparticles of varying size and crystal structure, rutile (15−20 nm), anatase (5−7 nm), and nanotubes, we observed alterations in cytokine expression, suggesting that all of the TiO_2 nanoparticle preparations inflame the PTE construct (Figure 3). In comparison to untreated or micrometer TiO_2, all nanoparticle formulations generated a significant increase in pro-

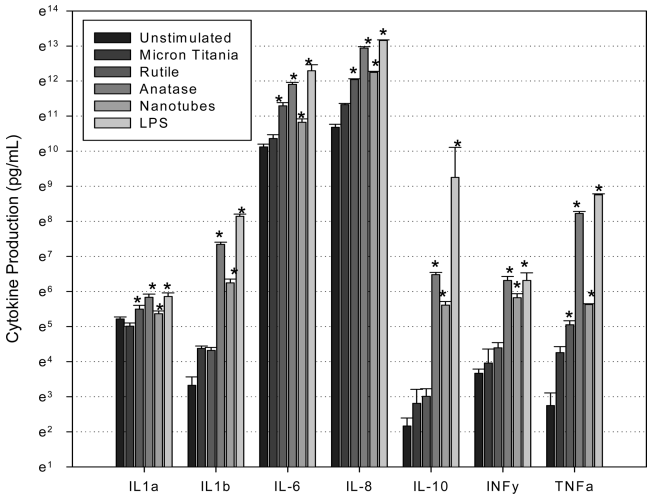

Figure 3. Nanoparticle treatment induces inflammatory cytokine production. The complete peripheral tissue equivalent module was treated with nanoparticles (1.56 μM) or LPS (10 ng/mL) for 24 h. Supernatant was harvested from each well and examined by cytokine luminex. Increased expression in proinflammatory cytokines in nanoparticle treatments over micrometer-sized titania was visualized across three donors with great consistency ((*) $p < 0.05$ as compared to micrometer titania). Error bars represent mean ± SD for at least three donors.

inflammatory cytokine secretion (5 to 20-fold) including IL-1α, IL-1β, IL-6, IL-8, IFNγ, and TNFα as seen across a cohort of at least five donors ($p < 0.05$). This is not surprising considering the complement of cytokines and chemokines monocytic cells typically produce when triggered by antigenic stimulation. Complementary to the monocytic cytokine milieu, the HUVEC monolayer has been characterized to be a major producer of IL-8 when under environmental stress such as the nanomaterial treatment. In addition to IL-8, the HUVEC also produce IL-6, a pleiotropic cytokine that plays an important role in host defense through immune and inflammatory regulation. In addition, immunosuppressive cytokine production was also elevated as compared to untreated and micrometer TiO_2. As seen *in vivo*, a balanced cytokine response is recapitulated in the PTE with the secretion of immunosuppressive cytokines like IL-10. The production of the immunosuppressive cytokine IL-10 by the resident phagocytic population in the PTE is likely an inflammatory mediator response to the increasing levels of IL-1 and TNFα.[29,30] The cytokine/chemokine data illustrate that nanoscale TiO_2 of different structures and associated surface chemistries induce an inflammatory response in the PTE construct. These data are corroborated by previous studies reporting ultrafine TiO_2 particles cause an increase in tissue inflammation and alter macrophage chemotactic response.[31] Together, this data concludes that at a dose of 1.56 μM, TiO_2 nanoparticles are reactive enough to initiate an inflammatory response.

Reactive Oxygen Species as a Component of Inflammation. Having shown that nanoparticles induce inflammatory responses within the PTE construct, we questioned which mechanisms of inflammation might be triggered by the materials. While it is unlikely that nanoparticles interact with toll-like receptors because they lack the conserved patterns found on viral and bacterial pathogens that trigger this pathway of the inflammatory response, TiO_2 is highly photoreactive and has the potential to generate reactive oxygen intermediates in biological systems. These intermediates have damaging effects upon cell viability and function, and, in turn, stimulate innate immune responses.[32] To detect the presence of reactive oxygen species (ROS) in the PTE after 48 h treatment with the nanoparticle preparations, we used a 2,7-dichlorofluorescein (DCF) assay. Briefly, nonfluorescent fluorescein derivatives (reduced dichlorofluorescein, DCFH) are placed into the culture medium, and after being oxidized by ROS, these compounds fluoresce. By quantifying total fluorescence, we were able to quantify the total ROS by flow cytometry. Figure 4 clearly shows a 10−20 fold increase in the ROS levels in PBMCs and HUVECs following 48-h treatment with the TiO_2 nanoparticles distinct from the micrometer titania, which resembles the untreated control profile. In addition, we investigated the constituent cell lineages of PBMCs (CD3, CD4, CD8, CD19, and CD14) to determine if any single subpopulation was biased toward production of ROS. Antibodies to the cell surface markers listed above were used to stain the nanoparticle-treated PBMCs that were subsequently analyzed by flow cytometry. We found that the greatest ratio of ROS producers were $CD14^+$ (monocytes), with over 80% of the total $CD14^+$ population positive for DCF expression (data not shown). Thus, it should be noted that the resulting increased ROS production is likely coming primarily from a cellular source (such as NADPH oxidase) and not directly from the chemical reactivity of titanium dioxide. However it is not yet clear whether low level ROS production, mediated through the chemistry or crystal structure of the nanoparticle, is responsible for triggering the ROS response by the monocytes. Nonetheless, this is consistent with previous findings that phagocytes are responsible for the majority of ROS generation in mounting an inflammatory response *in vivo*.[33−35] While the ROS generation between different nanoparticle architectures was not equivalent, it is difficult to state any correlation of ROS production linked to particle dimension. However, it is clear that the material properties of nanotitanium dioxide invoke a more pronounced level of ROS in both HUVEC and PBMCs beyond the null and micrometer titanium dioxide treated cultures, as previously reported in other culture models.[36] The absence of an increase in both proinflammatory cytokines and ROS in the micrometer titania treated cultures suggests the behavior of nanotitanium mediates a proinflammatory effect as previously reported with other nanomaterials.[37] However, ROS generation is not the only pathway to consider for the induction of an immune response to nano-

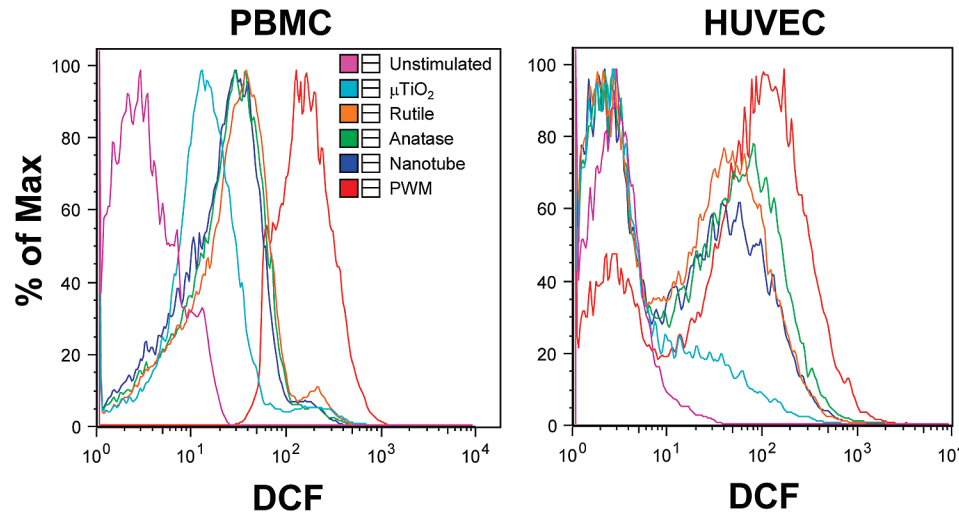

Figure 4. Nanoparticles induce ROS production in primary tissue culture models. HUVEC cells cultured in medium 199 containing 20% serum and PBMCs cultured in X-VIVO-15 were exposed to TiO_2 nanoparticles or PWM at concentrations indicated in the histograms. ROS production was assessed after a 24 h exposure. To properly assess ROS generation, the cells were washed of culture and condition media and stained briefly with DCF in PBS and immediately acquired by flow cytometry. DCF fluorescence was measured in the FITC channel. Analysis is gated on live cells only. Plots are representative of several independent experiments.

materials, it is likely that ROS participates in a conglomerate of steps that lead to innate immune activation. It is believed that activation of the inflammasome is a central feature to activating the innate immune system prior to the initiation of an effective adaptive immune response. Recent reports have concluded that nanoparticles may have the capacity to activate the inflammasome pathway *via* signaling both TLR and NLRP3 in antigen-presenting cells leading to the increased production of proinflammatory cytokine IL-1β.[38,39] The authors have observed such an increase in IL-1β (Figure 3) upon treatment with nanoparticles and propose to include in future studies an assessment of inflammasome activation in response to ROS and other "danger signals" as an alternative mechanism of innate immune activation by nanomaterials.

Effect of Nanoparticles on DC Maturation and Function. DCs are a unique antigen-presenting cell (APC) population that can both participate in inflammatory reactions, by producing a variety of inflammatory mediators, and directly respond to the product of these innate pathways by undergoing a process of maturation that allows them to become more potent inducers of the adaptive arm of the immune response. In the absence of stimuli, the vast majority of DCs are immature. Uptake and processing of antigen in combination with the aforementioned inflammatory signals matures them into potent DCs capable of initiating antigen-specific primary and secondary immune responses when combined with lymphocytes. It is unclear whether or not treatment with nanoparticles can trigger DC maturation, but the ability of nanoscale TiO_2 to induce ROS in phagocytes suggests the possibility that these materials might activate this potent APC population. Previous reports have described nanoparticle uptake by APCs, supporting the pathway of APC activation.[40]

DCs for research and clinical applications are typically derived from purified blood monocytes and are cultured in a cocktail of cytokines for a week or more.[41] The caveat being that these DCs are harvested as a highly synchronized and uniform population of cells, uncharacteristic of the DC populations found *in vivo*.[42] An asset of the PTE model is its ability to generate DCs without the use of exogenous factors, in a HUVEC-driven system, recapitulating their growth and diversity *in vivo*.[16] Within this construct, DC maturation can be tied to the increased expression of the activation markers, CD1a and CD83, similar to what is observed *in vivo*. Additionally, the expression of chemokine receptor complex CCR7 is associated with the control of immature and mature DC migration *in vivo*, and has been shown to increase on PTE-derived DCs following treatment of the construct with known inflammatory stimuli.[18,43,44]

Treatment of the PTE with nanoparticles generated a population shift from a precursor DC phenotype, traditionally $CD14^+$ and HLA-DR^+, to an increased number of immature and mature DC phenotype $CD14^-$/HLA-DR^{+low}, $CD14^-$/HLA-DR^{+high}, respectively.[16] Analysis of the nanoparticle TiO_2 stimulated $CD14^-$/HLA-DR^+ population demonstrated significantly enhanced expression of mature DC-specific marker CD83, secondary lymphoid tissue-directing chemokine receptor CCR7 and the costimulatory molecule CD86 compared to unstimulated and micrometer controls and was similar to cultures stimulated with LPS (Figure 5). There is an approximate 3-fold increase in DC-specific maturation marker CD83 expression on DCs treated with anatase, rutile, and nanotubes over those given micrometer-

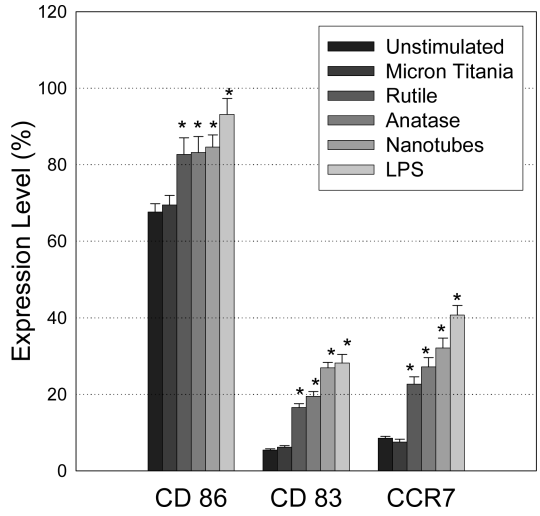

Figure 5. DCs increase expression of maturation markers upon stimulation with nanoparticles. The PTE was loaded with PBMCs which were incubated for 90 min to allow migration of the APC population. Nonmigrated cells were then removed and the cultures were incubated for 24 h. Nanoparticles were then applied at a concentration of 1.56 μM and subsequently incubated for 24 h. The reverse transmigratory (RT) fraction was then harvested and labeled with specific antibody. Treatment with nanotubes resulted in approximately 15% increase in maturation marker expression as compared to the micrometer titania treated cells ((*) $p < 0.05$ as compared to micrometer titania). Bars indicate expression level (mean fluorescent intensity, MFI) of surface proteins from the migrated RT fraction. Analysis includes only live gated monocytes. Error bars represent mean ± SD for at least three donors.

sized titania ($p < 0.05$). This shift can be explained by inflammation of the resident DC population from phagocytosis and exposure to soluble nanoparticles and perhaps synergy with the inflamed endothelial cells in the PTE. The increase in CD86 and CCR7 indicate the DCs maturing ability for the costimulation of lymphocytes, triggering their subsequent activation and proliferation as seen *in vivo*, further suggesting the potential to drive such an adaptive response.

Nanoparticle-Pulsed DCs Efficiently Prime Allogeneic Naïve CD4$^+$ T Cells. The capacity of nanoparticle-pulsed DCs to activate allogeneic naïve CD4$^+$ T cells (CD45RA$^+$CD45RO$^-$) was assessed by carboxyfluorescein succinimidyl ester (CFSE) dilution and CD25$^+$ expression (Figure 6). Activation of T cells will lead to the upregulation of CD25 surface expression and to proliferation of these cells as measured by CFSE diminution. Indeed, DCs treated with nanoparticles were powerful stimulators of naïve CD4$^+$ T cell proliferation and CD25 expression. Panel A shows the basal level of activation in the untreated control compared to those treated with phytohemagglutinin/phorbol myristate acetate (PHA/PMA) in the absence of DCs. Panels B and C both show the proliferative response with the addition of DCs to the T cells. DCs were either unpulsed or pulsed with nanomaterials or given a maturation cocktail of TNFα and PGE_2. The proliferative activation of the T cells primed with nanomaterial pulsed DCs mimics the response of the T cells primed with matured DCs. Thus, TiO_2 nanomaterials are powerful inducers of naïve CD4$^+$ T-cell proliferation.

This investigation assessed the immunogenicity of nanostructured TiO_2 through the use of a model of human immunity, the MIMIC system. Currently, the literature is divergent on the biocompatibility of nanostructured TiO_2. Previous studies suggesting the biocompatibility of these particles have been established through growth and viability assays of primary or cancer lines where nanostructured TiO_2 provides a biomemetic support as a film or other coating. Indeed, physical analysis of nanostructured TiO_2 films revealed a granularity and porosity that mimics the natural extracellular matrix; such nanotopography has repeatedly been shown to enhance cell adhesion making TiO_2 films a suitable substrate for cell-based and tissue-based applications as mentioned in the introduction.[1,4] However, the behavior of nanostructured TiO_2 as a thin film may be vastly different than that of free particulate nanostructured TiO_2. This study adds to previous reports that have shown TiO_2 nanoparticles to be cyto/genotoxic and immunogenic when delivered into animal or cell culture models.[13,45] Cumulatively, these studies represent a schism in nanostructured TiO_2 biocompatibility. We have investigated nanoparticles using an alternative approach focused on human immunity that we believe has illuminated some of the controversy of TiO_2 biocompatibility. Our data has shown TiO_2 nanoparticles generate an immune response through the confluence of increased proinflammatory cytokine production and ROS generation. These precursory steps of activation assist in DC maturation upon exposure to these nanoparticles and facilitates the functionality of the nanoparticle pulsed DCs to activate naïve CD4$^+$ T cells and initiate lymphoproliferation. The lack of response above unstimulated control from the micrometer-sized TiO_2 particles coupled with the data from studies on nanostructured film suggest that larger particles, or those that have been cluster-assembled, remain inert and biocompatible while free TiO_2 nanoparticles may represent a health hazard.

Utilization of the MIMIC system has shown that nanoscale TiO_2 can initiate a cascade of events from activation of the endothelium to produce proinflammatory cytokines which lead to the maturation of resident DCs that, in turn, can regulate effector cell responses. This may seem confounding when compared to previous studies which have shown cells cannot specifically target materials that lack a protein recognition motif.[46] However, it has been shown more recently that TiO_2 antigens may be formed based on protein binding to TiO_2 nanoparticles, potentially influencing their activity *in vivo*.[47] The data above display that nanomaterials can activate DCs, even if only in a nonspecific inflammatory manner, which has major implications for autoim-

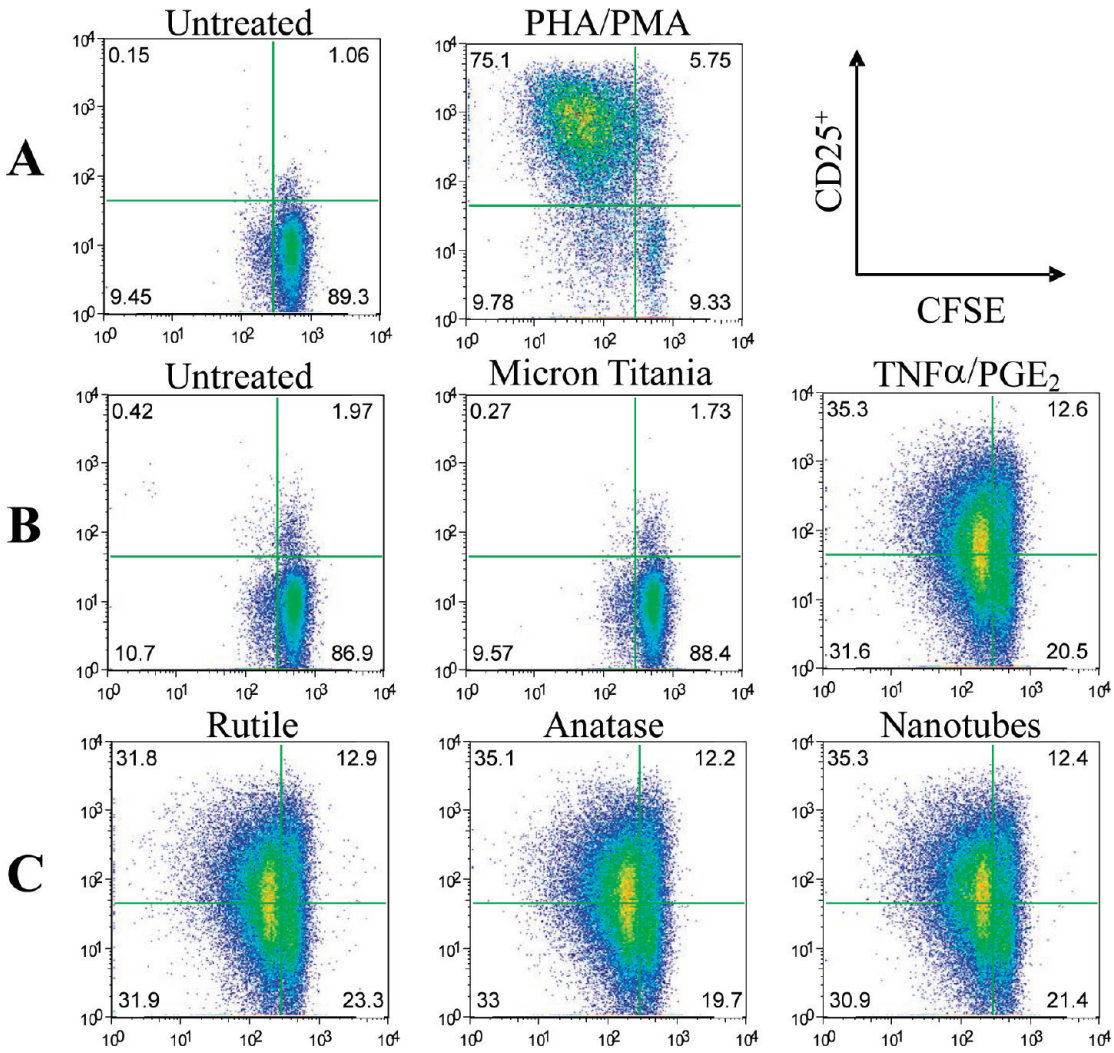

Figure 6. Nanoparticle-treated DCs induced proliferation of allogeneic Naïve $CD4^+$ T Cells. (A) Naïve $CD4^+$ T cells were untreated or stimulated with PHA and PMA in the absence of DCs. Control (B) naïve $CD4^+$ T cells, primed with HUVEC-derived DCs pulsed with nanomaterials for 48 h (C), were cultured for 5 days. Proliferative response and T-cell activation were determined by FACS as a measure of CFSE dilution and $CD25^+$ expression, respectively. Data are representative of five donors.

mune induction and instigating allergic reactivity. However, our studies also demonstrate that these nanomaterials may perform as effective adjuvants for use in vaccines because they have the capacity to not only stimulate the innate response but also initiate the adaptive arm through their interactions with DCs. The use of the *in vitro* human immune model (MIMIC system) on these sets of TiO_2 nanomaterials has revealed their inflammatory potential; and may provide an immunological platform with broad application capable to rapidly evaluate a wide range of chemicals and materials in a physiologically relevant manner. This tool may find applications for the broader nanoscience and environmental science community to accurately address potential concerns over the immunotoxicology of nanomaterials.

MATERIALS AND METHODS

Materials. Bacterial lipopolysaccharide (LPS) and pokeweed mitogen (PWM) were obtained from Sigma (St. Louis, MO). The tetrazolium dye, 3-[4,5-dimethylthiazol-2-yl]-2,5-diphenyl tetrazolium bromide (MTT) was obtained from Invitrogen (Carlsbad, CA). Silicone dioxide nanoparticles (used as a comparative control in some experimental models) were obtained from Sigma. Reactive oxygen species (ROS) levels were determined using 2′,7′-dichlorodihydrofluorescein diacetate (DCF; Sigma).

Synthesis of Titania Nanoparticles. Nanoparticles were synthesized by wet chemical synthesis. At first a 50:50 mixture of ethanol (99.8% Sigma Aldrich) and deionized water (18.2 M) was boiled to reflux. At this point the pH of the boiling solution was adjusted to pH 3.0 by the addition of 1 N HCl. Titanium isopropoxide (Sigma Aldrich) was added slowly to this refluxing mixture which precipitates immediately to a white solution. The solution was then stirred at 85 °C for 4 h. The white solution was then cooled to room temperature and washed several times with ethanol until dry. The as prepared sample was mostly anatase (partially amorphous) and was used as such. For obtaining rutile nanoparticles the anatase nanoparticles were calcined at 800 °C for 2 h and the crystalline structure was confirmed using X-ray diffraction.

Synthesis of Titania Nanotubes. Titania nanotubes were prepared by hydrothermal procedure previously established.[48,49] In a typical synthesis 0.5 g of anatase titania from above synthesis was mixed with 20 mL of 10 M sodium hydroxide solution. The mix was then poured in an autoclave and heated at various temperatures from 120−150 °C for 20−24 h. The final solution was cooled to room temperature and washed several times to remove additional sodium hydroxide. A final wash of 1 N HCl to neutralize was carried out and titania nanotubes (partially amorphous) were subsequently washed again several times, filtered, and dried at 120 °C. Nanoparticles were dispersed in Dulbecco's phosphate buffered saline (DPBS; Lonza, Basel, Switzerland) by sonication and vortexing followed by immediate delivery to the cultures.

Transmission Electron Microscopy. The samples were analyzed using high resolution transmission electron microscopy (HRTEM) (Philips 300 TECNAI operated at 300 kV) to confirm the shape, size and morphology of the nanoparticles. The samples were prepared by dipping a polycarbon-coated copper grid into a dilute suspension of nanoparticles dispersed in acetone.

Evaluation of Endotoxin Contamination. All nanoparticles samples were analyzed for the presence of endotoxin contamination using a quantitative kinetic chromogenin Limulus Amoebocyte Lysate method (Lonza-BioWitthaker, Walkersville, MD). *Escherichia coli* 055:B5 endotoxin (Lonza BioWitthaker) was used as a standard.

Human Peripheral Blood Mononuclear Cell Isolation. Aphaeresis was performed at Florida's Blood Center (Orlando, FL) using a COBE Spectra Apheresis System (Gambro, Lakewood, CO). The study was reviewed and approved by the Chesapeake Research Review Inc. (Columbia, MD). All donors were in good health and were negative for blood-borne pathogens as detected by standard blood bank assays. The aphaeresis product was processed to enrich the peripheral blood mononuclear cell (PBMC) fraction by using ficoll-hypaque (Amersham, Piscataway, NJ) density gradient separation according to standard protocols as previously described.[19] PBMCs were cryopreserved in DMSO-containing media for extended storage in liquid nitrogen vapor phase until needed.

Cell Culture. The two primary cell types were used in this study are human umbilical vein endothelial cells (HUVEC; Lonza) and PBMCs. HUVECs have been shown to be intimately involved in orchestrating the inflammatory cell response *via* transendothelial cell trafficking, making them a suitable choice for this coculture model. HUVEC were cultured as previously described.[50] PBMC aliquots were thawed in Iscoves Modified Dulbecco's medium (Lonza) supplemented with 10% autologous donor serum, 100 IU/mL penicillin and 100 μg/mL streptomycin. Cells were washed and cultured in X-VIVO-15 (Lonza) seeded into 24-well dishes at 2.5×10^6 cells per well. All cultures were incubated at 37 °C in a humidified incubator with 5% CO_2.

Cell Viability Assay. To determine toxicity levels of nanoparticles, HUVEC and PBMCs cultures were prepared at approximately 2000 and 20000 cells per well, respectively, in 96-well flat bottom tissue culture plates. The HUVEC monolayer was approximately 70−80% confluent after 24 h of culture. Serial dilutions of rutile, anatase, and titania nanotubes were added and incubated 24 h. MTT was added to each well (1.2 mM) and incubated for 4 h at 37 °C with 5% CO_2. To solubilize the dye, a cell lysis solution (10% SDS, 5 mM HCl) was added and incubated for 14 h at 37 °C. Absorbance of the soluble dye was determined at 570 nm in using a Spectramax 190 UV−visible spectrophotometer (Molecular Devices, Sunnyvale, CA). To validate the use of this assay on these cell types as a representative measure of cell viability, we used a standard curve of known concentration of cells (established by counting trypan blue stained cells with a heamocytometer). In addition, HUVEC and PBMCs cultures were prepared at approximately 2000 and 20000 cells per well, respectively, in 96-well flat bottom tissue culture plates as described above. LDH release was monitored using a Spectramax 190 UV−visible spectrophotometer (Molecular Devices, CA) as described by the manufacturer (Roche, Basel, Switzerland) to acquire additional information about the cytotoxicity of the nanoparticle treatment.

ROS Determination. HUVECs were cultured in 24-well flat bottom tissue culture plates until 70−80% confluent. PBMCs were cultured into 24-well dishes at a density of 2×10^6 cells per well. The cultures were then treated with serial dilutions of rutile, anatase, and titania nanotubes for 48 h. Subsequently, cultures were treated at room temperature for 30 min with DCF at a final concentration of 10 μM. Cells were washed of excess dye with DPBS, harvested using cell dissociation solution (Sigma), and washed again in DPBS. Fluorescence of the oxidized DCF (indicative of peroxide levels) was analyzed by flow cytometry using LSR II (BD Pharmingen, San Diego, CA). FlowJo software (Treestar, Ashland, OR) was used for data analysis.

Allogeneic Naive $CD4^+$ T-Cell Proliferation. DCs were derived from the HUVEC-based model and were stimulated with the TiO_2 particle preparations (micrometer TiO_2, rutile, or nanotubes) (1.56 μM) for 48 h. The DCs were harvested and added at an optimized ratio of 1:400 to allogeneic naïve $CD4^+$ T cells previously isolated by magnetic separation (Miltenyi Biotec) and labeled with carboxyfluorescein succinimidyl ester (CFSE) following the instructions of the manufacturer (Molecular Probes, Invitrogen). As a positive control of proliferation and activation, phytohemagglutinin and phorbol 12-myristate 13-acetate (PHA/PMA) (1 μg/mL each) was added to wells containing only the $CD4^+$ cells and as a negative control the $CD4^+$ were unstimulated. After five days the cultures were harvested and stained following the manufacturers instruction for CD25, CD3, CD4, (eBioscience) and Live/Dead Aqua for viability (Invitrogen) and then acquired by flow cytometry using BD Pharmingen's LSR II.

Dendritic Cell Phenotyping. Phycoerythrin (PE), allophycocyanin (APC), Peridinin chlorophyll protein (PerCP-Cy5.5)-conjugated monoclonal antibodies specific for human CD14 (M5E2), CD86 (2331), CD83 (HB15e), CCR7, and HLA-DR (L243) (all from BD Pharmingen) were used to determine the cell surface receptors expressed on the reverse transmigratory DCs. Isotype control antibodies included MIgG2a (G155-178) and MIgG1 (MOPC-21) were also purchased from BD Pharmingen. DCs from the PTE module were collected and labeled with the above-mentioned specific antibodies for 45 min at 4 °C in PBS containing 2% bovine serum albumin (BSA) and 0.05% sodium azide, washed extensively, and cells were subsequently fixed with 2% paraformaldehyde. Flow cytometry was used to determine the abundance of each cell type (subpopulation) expressing markers using LSRII (BD Pharmingen) and FlowJo software (Treestar) as described above.

Bioplex Cytokine Quantification Assay. Supernatant samples collected from the PTE-MIMIC module were analyzed for cytokine production by means of the BIOPLEX Multiplexing array system (Bio-Rad, Hercules, CA) as previously described.[51] Samples were harvested after 48 h of treatment with nanoparticles or positive control antigens.

Peripheral Tissue Equivalent Module. The peripheral tissue equivalent (PTE) was prepared as previously described.[16] HUVEC monolayers were seeded with 5×10^5 PBMCs per well in a 96-well format. After a 90 min migration period, the excess PBMCs were washed from the module. Treatments of TiO_2 nanoparticles (1.56 μM) or LPS (10 ng/mL) were immediately applied and allowed to incubate for 48 h. The RT APC were then harvested at the 48 h time point and analyzed by DC phenotyping while the supernatants were examined for cytokine production using the BioPlex system.

Statistical Analysis. Each experiment was confirmed at least three times using cells isolated from at least three separate donors. All results were analyzed using analysis of variance (ANOVA). Statistical significance was considered at $p < 0.05$.

Acknowledgment. Vaxdesign's contribution was funded by the DARPA/Defense Sciences Office RVA Phase II Program and the work performed at UCF was funded by NSF Grant CBET-0711239 to S.S. and W.S.

REFERENCES AND NOTES

1. Carbone, R.; Marangi, I.; Zanardi, a.; Giorgetti, L.; Chierici, E.; Berlanda, G.; Podesta, a.; Fiorentini, F.; Bongiorno, G.; Piseri,

P.; *et al*. Biocompatibility of Cluster-Assembled Nanostructured TiO_2 with Primary and Cancer Cells. *Biomaterials* **2006**, *27*, 3221–9.
2. Rasmusson, L.; Roos, J.; Bystedt, H. A 10-Year Follow-up Study of Titanium Dioxide-Blasted Implants. *Clin. Implant Dent. Relat. Res.* **2005**, *7*, 36–42.
3. Chen, F.; Lam, W. M.; Lin, C. J.; Qiu, G. X.; Wu, Z. H.; Luk, K. D.; Lu, W. W. Biocompatibility of Electrophoretical Deposition of Nanostructured Hydroxyapatite Coating on Roughen Titanium Surface: *In Vitro* Evaluation Using Mesenchymal Stem Cells. *J Biomed. Mater. Res., B* **2007**, *82*, 183–91.
4. Liu, X.; Zhao, X.; Fu, R. K.; Ho, J. P.; Ding, C.; Chu, P. K. Plasma-Treated Nanostructured TiO(2) Surface Supporting Biomimetic Growth of Apatite. *Biomaterials* **2005**, *26*, 6143–50.
5. Annesi-Maesano, I.; Dab, W. Air Pollution and The Lung: Epidemiological Approach. *Med. Sci. (Paris)* **2006**, *22*, 589–94.
6. Auger, F.; Gendron, M. C.; Chamot, C.; Marano, F.; Dazy, A. C. Responses of Well-Differentiated Nasal Epithelial Cells Exposed to Particles: Role of the Epithelium in Airway Inflammation. *Toxicol. Appl. Pharmacol.* **2006**, *215*, 285–94.
7. Brunekreef, B.; Holgate, S. T. Air Pollution and Health. *Lancet* **2002**, *360*, 1233–42.
8. Lin, W.; Huang, Y. W.; Zhou, X. D.; Ma, Y. Toxicity of Cerium Oxide Nanoparticles in Human Lung Cancer Cells. *Int. J. Toxicol.* **2006**, *25*, 451–7.
9. Oberdorster, G.; Gelein, R. M.; Ferin, J.; Weiss, B. Association of Particulate Air Pollution and Acute Mortality: Involvement of Ultrafine Particles? *Inhal. Toxicol.* **1995**, *7*, 111–24.
10. Wildhaber, J. H. Aerosols: The Environmental Harmful Effect. *Paediatr. Respir. Rev.* **2006**, *7*, S86–7.
11. Baan, R.; Straif, K.; Grosse, Y.; Secretan, B.; El Ghissassi, F.; Cogliano, V. Carcinogenicity of Carbon Black, Titanium Dioxide, and Talc. *Lancet Oncol.* **2006**, *7*, 295–6.
12. Baan, R. A. Carcinogenic Hazards From Inhaled Carbon Black, Titanium Dioxide, and Talc not Containing Asbestos or Asbestiform Fibers: Recent Evaluations by an IARC Monographs Working Group. *Inhal. Toxicol.* **2007**, *19*, 213–28.
13. Wang, J.; Chen, C.; Liu, Y.; Jiao, F.; Li, W.; Lao, F.; Li, Y.; Li, B.; Ge, C.; Zhou, G.; *et al*. Potential Neurological Lesion After Nasal Instillation of TiO(2) Nanoparticles in the Anatase and Rutile Crystal Phases. *Toxicol. Lett.* **2008**, *183*, 72–80.
14. Nel, A. E.; Diaz-Sanchez, D.; Ng, D.; Hiura, T.; Saxon, A. Enhancement of Allergic Inflammation by the Interaction Between Diesel Exhaust Particles and the Immune System. *J. Allergy Clin. Immunol.* **1998**, *102*, 539–54.
15. Xia, T.; Li, N.; Nel, A. E. Potential Health Impact of Nanoparticles. Annu. Rev. Public Health **2009**, *30*.
16. Randolph, G. J.; Beaulieu, S.; Lebecque, S.; Steinman, R. M.; Muller, W. A. Differentiation of Monocytes into Dendritic Cells in a Model of Transendothelial Trafficking. *Science* **1998**, *282*, 480–3.
17. Randolph, G. J.; Beaulieu, S.; Pope, M.; Sugawara, I.; Hoffman, L.; Steinman, R. M.; Muller, W. A. A Physiologic Function for P-Glycoprotein (MDR-1) During the Migration of Dendritic Cells from Skin *via* Afferent Lymphatic Vessels. *Proc. Natl. Acad. Sci. U.S.A.* **1998**, *95*, 6924–9.
18. Randolph, G. J.; Sanchez-Schmitz, G.; Liebman, R. M.; Schakel, K. The CD16(+) (FcgammaRIII(+)) Subset of Human Monocytes Preferentially Becomes Migratory Dendritic Cells in a Model Tissue Setting. *J. Exp. Med.* **2002**, *196*, 517–27.
19. Schanen, B. C.; Drake, D. R.,. III. A Novel Approach for the Generation of Human Dendritic Cells from Blood Monocytes in the Absence of Exogenous Factors. *J. Immunol. Methods* **2008**, *335*, 53–64.
20. Erli, H. J.; Ruger, M.; Ragoss, C.; Jahnen-Dechent, W.; Hollander, D. A.; Paar, O.; von Walter, M. The Effect of Surface Modification of a Porous TiO_2/Perlite Composite on the Ingrowth of Bone Tissue *in Vivo*. *Biomaterials* **2006**, *27*, 1270–6.
21. Karpagavalli, R.; Zhou, A.; Chellamuthu, P.; Nguyen, K. Corrosion Behavior and Biocompatibility of Nanostructured TiO_2 Film on Ti6Al4 V. *J. Biomed. Mater. Res., A* **2007**, *83*, 1087–95.
22. Popat, K. C.; Leoni, L.; Grimes, C. A.; Desai, T. A. Influence of Engineered Titania Nanotubular Surfaces on Bone Cells. *Biomaterials* **2007**, *28*, 3188–97.
23. Warheit, D. B.; Webb, T. R.; Reed, K. L.; Frerichs, S.; Sayes, C. M. Pulmonary Toxicity Study in Rats with Three Forms of Ultrafine-TiO_2 Particles: Differential Responses Related to Surface Properties. *Toxicology* **2007**, *230*, 90–104.
24. Warheit, D. B.; Webb, T. R.; Sayes, C. M.; Colvin, V. L.; Reed, K. L. Pulmonary Instillation Studies with Nanoscale TiO_2 Rods and Dots in Rats: Toxicity Is Not Dependent Upon Particle Size and Surface Area. *Toxicol. Sci.* **2006**, *91*, 227–36.
25. Goto, K.; Tamura, J.; Shinzato, S.; Fujibayashi, S.; Hashimoto, M.; Kawashita, M.; Kokubo, T.; Nakamura, T. Bioactive Bone Cements Containing Nano-Sized Titania Particles for Use as Bone Substitutes. *Biomaterials* **2005**, *26*, 6496–505.
26. Chung, C. J.; Lin, H. I.; Tsou, H. K.; Shi, Z. Y.; He, J. L. An Antimicrobial TiO_2 Coating for Reducing Hospital-Acquired Infection. *J. Biomed. Mater. Res., B* **2008**, *85*, 220–4.
27. Kapetanovic, R.; Cavaillon, J. M. Early Events in Innate Immunity in the Recognition of Microbial Pathogens. *Expert Opin. Biol. Ther.* **2007**, *7*, 907–18.
28. van Vliet, S. J.; den Dunnen, J.; Gringhuis, S. I.; Geijtenbeek, T. B.; van Kooyk, Y. Innate Signaling and Regulation of Dendritic Cell Immunity. *Curr. Opin. Immunol.* **2007**, *19*, 435–40.
29. D'Elia, R.; Else, K. J. *In Vitro* Antigen Presenting Cell-Derived IL-10 and IL-6 Correlate with *Trichuris muris* Isolate-Specific Survival. *Parasite Immunol.* **2009**, *31*, 123–31.
30. Harizi, H.; Gualde, N. Pivotal Role of PGE2 and IL-10 in the Cross-Regulation of Dendritic Cell-Derived Inflammatory Mediators. *Cell Mol. Immunol.* **2006**, *3*, 271–7.
31. Afaq, F.; Abidi, P.; Matin, R.; Rahman, Q. Activation of Alveolar Macrophages and Peripheral Red Blood Cells in Rats Exposed to Fibers/Particles. *Toxicol. Lett.* **1998**, *99*, 175–82.
32. Matsuzawa, A.; Saegusa, K.; Noguchi, T.; Sadamitsu, C.; Nishitoh, H.; Nagai, S.; Koyasu, S.; Matsumoto, K.; Takeda, K.; Ichijo, H. ROS-Dependent Activation of the TRAF6-ASK1-p38 Pathway Is Selectively Required for TLR4-Mediated Innate Immunity. *Nat. Immunol.* **2005**, *6*, 587–92.
33. Aukrust, P.; Muller, F.; Froland, S. S. Enhanced Generation of Reactive Oxygen Species in Monocytes From Patients with Common Variable Immunodeficiency. *Clin. Exp. Immunol.* **1994**, *97*, 232–8.
34. Park, E. J.; Park, K. Oxidative Stress and Pro-inflammatory Responses Induced by Silica Nanoparticles *in Vivo* and *in Vitro*. *Toxicol. Lett.* **2009**, *184*, 18–25.
35. Takahashi, M.; Nagao, T.; Imazeki, Y.; Matsuzaki, K.; Minamitani, H. Roles of Reactive Oxygen Species in Monocyte Activation Induced by Photochemical Reactions During Photodynamic Therapy. *Front Med. Biol. Eng.* **2002**, *11*, 279–94.
36. Reeves, J. F., Davies, S. J., Dodd, N. J. F., Jha, A. N., Hydroxyl Radicals Are Associated with Titanium Dioxide Nanoparticle Induced Cytotoxicity and Oxidative DNA Damage in Fish Cells. Mutat. Res. **2008**, *640*, 113−22.
37. Soto, K. F.; Murr, L. E.; Garza, K. M. Cytotoxic Responses and Potential Respiratory Health Effects of Carbon and Carbonaceous Nanoparticulates in the Paso del Norte Airshed Environment. *Int. J. Environ. Res. Public Health* **2008**, *5*, 12–25.
38. Demento, S. L.; Eisenbarth, S. C.; Foellmer, H. G.; Platt, C.; Caplan, M. J.; Mark Saltzman, W.; Mellman, I.; Ledizet, M.; Fikrig, E.; Flavell, R. A.; Fahmy, T. M. Inflammasome-Activating Nanoparticles as Modular Systems for Optimizing Vaccine Efficacy. *Vaccine* **2009**, *27*, 3013–21.
39. Sharp, F. A.; Ruane, D.; Claass, B.; Creagh, E.; Harris, J.; Malyala, P.; Singh, M.; O'Hagan, D. T.; Petrilli, V.; Tschopp, J.;

et al. Uptake of Particulate Vaccine Adjuvants by Dendritic Cells Activates the NALP3 Inflammasome. *Proc. Natl. Acad. Sci. U.S.A.* **2009**, *106*, 870–5.
40. Moss, O. R.; Wong, V. A. When Nanoparticles Get in the Way: Impact of Projected Area on *in Vivo* and *in Vitro* Macrophage Function. *Inhal. Toxicol.* **2006**, *18*, 711–6.
41. Pickl, W. F.; Majdic, O.; Kohl, P.; Stockl, J.; Riedl, E.; Scheinecker, C.; Bello-Fernandez, C.; Knapp, W. Molecular and Functional Characteristics of Dendritic Cells Generated from Highly Purified CD14+ Peripheral Blood Monocytes. *J. Immunol.* **1996**, *157*, 3850–9.
42. Kohl, K.; Schnautz, S.; Pesch, M.; Klein, E.; Aumailley, M.; Bieber, T.; Koch, S. Subpopulations of Human Dendritic Cells Display a Distinct Phenotype and Bind Differentially to Proteins of the Extracellular Matrix. *Eur. J. Cell Biol.* **2007**, *86*, 719–30.
43. Banchereau, J.; Steinman, R. M. Dendritic Cells and the Control of Immunity. *Nature* **1998**, *392*, 245–52.
44. Randolph, G. J.; Inaba, K.; Robbiani, D. F.; Steinman, R. M.; Muller, W. A. Differentiation of Phagocytic Monocytes into Lymph Node Dendritic Cells *in Vivo*. *Immunity* **1999**, *11*, 753–61.
45. Wang, J. J.; Sanderson, B. J.; Wang, H. Cyto- and Genotoxicity of Ultrafine TiO_2 Particles in Cultured Human Lymphoblastoid Cells. *Mutat. Res.* **2007**, *628*, 99–106.
46. Godfrey, D. I.; Rossjohn, J.; McCluskey, J. The Fidelity, Occasional Promiscuity, and Versatility of T-Cell Receptor Recognition. *Immunity* **2008**, *28*, 304–14.
47. Vamanu, C. I.; Hol, P. J.; Allouni, Z. E.; Elsayed, S.; Gjerdet, N. R. Formation of Potential Titanium Antigens Based on Protein Binding to Titanium Dioxide Nanoparticles. *Int. J. Nanomed.* **2008**, *3*, 69–74.
48. Yao, Z.; Braidy, N.; Botton, G. A.; Adronov, A. Polymerization from the Surface of Single-Walled Carbon Nanotubes—Preparation and Characterization of Nanocomposites. *J. Am. Chem. Soc.* **2003**, *125*, 16015–24.
49. Zhang, S.; Peng, L. M.; Chen, Q.; Du, G. H.; Dawson, G.; Zhou, W. Z. Formation Mechanism of $H_2Ti_3O_7$ Nanotubes. *Phys. Rev. Lett.* **2003**, *91*, 256103.
50. Muller, W. A.; Randolph, G. J. Migration of Leukocytes across Endothelium and Beyond: Molecules Involved in the Transmigration and Fate of Monocytes. *J. Leukoc. Biol.* **1999**, *66*, 698–704.
51. Penolazzi, L.; Lambertini, E.; Tavanti, E.; Torreggiani, E.; Vesce, F.; Gambari, R.; Piva, R. Evaluation of Chemokine and Cytokine Profiles in Osteoblast Progenitors from Umbilical Cord Blood Stem Cells by BIO-PLEX Technology. *Cell Biol. Int.* **2008**, *32*, 320–5.